Fundamental Acoustic Finger Force for Out-of-Plane Ultrasonic Vibration and its Correlation with Friction Reduction

Diana Angelica Torres, Anis Kaci, Frederic Giraud, Christophe Giraud-Audine, Michel Amberg, Stephane Clenet, Betty Lemaire-Semail

Fundamental Acoustical Finger Force Calculation for Out-of-Plane Ultrasonic Vibration and its Correlation with Friction Reduction

(Revised March 2020)

Angelica Torres, Anis Kaci, Frederic Giraud, *Member, IEEE*, Christophe Giraud-Audine, *Member, IEEE*, Michel Amberg, Stephane Clenet, *Member, IEEE*, and Betty Lemaire-Semail, *Member, IEEE*

Abstract—When a finger touches an ultrasonic vibrating plate, a non-sinusoidal contact force is produced. This force is denominated acoustical finger force. In this paper, a method is proposed, in order to observe its fundamental component in the context of a friction reduction haptic interface. A PCA (Principal Component Analysis) is applied to the measured data, which will help evaluate the correlation between this measurement and the friction when sliding the finger. A linear model that predicts the friction coefficient is laid down and evaluated. The interest of this study is to provide a mean to adapt the tactile feedback device control to each user, despite of the biomechanical properties differences within each finger pad.

Index Terms— Force, Friction, Vibrations, Acoustic measurements, Mathematical model, Skin, Damping, PCA

1 Introduction

ULTRASONIC out-of-plane vibration is one of the leading technologies to create friction modulation in haptic surfaces. By modulating the friction forces between a vibrating plate and a user's finger as a function of its position, illusions of out of plane shapes and textural patterns can be created [1], [2]. The intermittent contact between the finger pad and the plate, that occurs during out-of plane vibrations at amplitudes as low as few micrometers, is at the origin of the friction reduction [3], [4]. It has been observed that the finger biomechanics may be used to predict the behavior of friction forces during tactile surface exploration. In [3], it is shown that soft stratum-corneum -- with a low Young modulus -- has lower friction reduction, while [5] has established that the damping of the stratum corneum at ultrasonic frequencies greatly affects the subject's susceptibility to ultrasonic friction modulation.

Therefore, it is conceivable that certain finger mechanical properties are correlated to a measure of the textural perception. This is further supported by [6], which has shown that the perceptual intensity of the tactile stimuli is a function of the friction contrast. This has been confirmed by [7], where this intensity is modelled by introducing as well the rate of change of the tangential force. A difference between falling and rising friction is observed, which is due to the viscoelastic properties of the fingertip.

Hence, to obtain a same perceptual intensity of a tactile stimulus, the vibration amplitude should be adapted according to the scanning speed and pressing force, which can be measured with sensors, but also to the biomechanical properties of the finger pad, which change from one user to another. A previous attempt has been performed in [14], using a real time friction sensor integrated in the tactile feedback surface, but the feedback signal was noisy and difficult to use in a lose loop control. In [8], the measured acoustical impedance is correlated to the perception of simulated keyclick, since this parameter is directly correlated to the biomechanical properties of the finger pad. The authors propose to use this measurement as a monitoring tool to produce a calibrated stimulation to each user.

In this paper, a similar objective is targeted: how to adapt the friction stimulation to each user. In our case, we wish to use the measurement of the acoustic forces in the case of friction reduction tactile displays. For that purpose, we first present the principle of an online measurement of the forces. We then present an experimental study which aims to correlate the force measurement to the friction reduction. The results of this study are then analyzed using PCA (Principal Component Analysis), and the results are presented in the final section showing a coreation between friction contrast [6] and acoustical finger force.

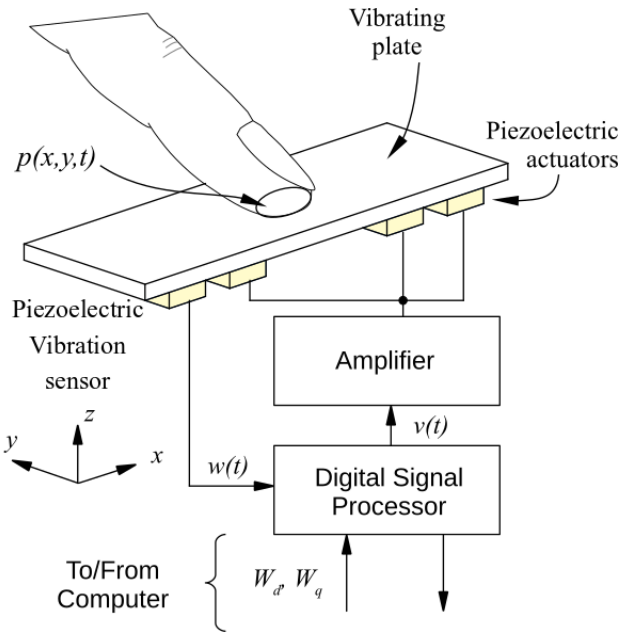

Figure 1. Principle of the acoustical force measurement.

2 PRINCIPLE OF THE FUNDAMENTAL ACOUSTICAL FORCE MEASUREMENT

2.1 Definition of the acoustical finger force

We consider figure 1, a vibrating plate which is actuated by piezoelectric patches powered by a voltage $v(t)$ around a pulsation denoted ω, and whith vibration amplitude $w(t) = Wsin(\omega t)$, whith W ranging between 0 and $2\mu m_{p-p}$.

The voltage $v(t)$ creates a deformation force f_p in the piezoelectrics, such that $f_p = Nv(t)$, with N being a parameter of the system named the conversion factor [1].

In general, the dynamic system of the plate can be described as in equation (5), with M, D and K representing the modal mass, damping and elasticity of the plate, respectively [1]. If this equation is represented in the Laplace domain, it takes the form (5). In the imaginary plane, $s = j\omega$. In that case, it is possible to obtain equation (5). At resonance, $\omega = \omega_n$ with $\omega_n = \sqrt{K/M}$. In that case, equation (5) becomes (5). f_p is therefore used to compensate the internal friction force that exists due to the plate's particles motion (internal damping).

$$f_p = M\ddot{w} + D\dot{w} + Kw \quad (1)$$

$$f_p = Mws^2 + Dws + Kw \quad (2)$$

$$f_p = (K - M)\omega^2 + j\omega Dw \quad (3)$$

$$f_p = D\dot{w} \quad (4)$$

When a finger touches the vibrating plate, contact forces appear that can create additional damping and stiffness into the system formed by the plate and the finger. As a result, the voltage $v(t)$ needs to be adapted, so that f_p can also compensate the effect of the contact forces on the vibration, and maintain W constant [2]. Therefore, the voltage difference between the no-load condition and the contact condition is related to the contact forces, and thus to the biomechanical properties of the fingertip.

Without lack of generality, we consider the model of a vibrating plate which is operated exactly at its resonance frequency, leading to equation (5):

$$f_p - f_r = D\dot{w} \quad (5)$$

With D the internal damping of the plate around a resonance pulsation, and f_r, the acoustical force. In general, f_r derives from the contact pressure $P(x, y, t)$ which depends on time t, position $\{x, y\}$, and on the skin bio-mechanical properties (for this study, it is assumed that the squeeze film effect [3] affects the acoustic force measurement less than the intermittent contact, and does not depend on the bio-mechanical properties of the finger. For this reason it is not considered).

The theory of vibrational mechanics helps writing the relationship between f_r and P for a plate, by introducing $\Psi(x, y)$, the modal shape of the plate when vibrating

$$f_r = \int_S P(x, y, t)\Psi(x, y) \quad (6)$$

It is possible to observe f_r by inverting the relation (5), leading to (5).

$$\tilde{f}_r = Nv - D\dot{w} \quad (7)$$

Where $\tilde{f}_r$ represents an observation of f_r. It should be emphasized here that the acoustical finger force is the force which is due to the intermittent contact between the finger and the vibrating plate. Its fundamental is the frequency component corresponding to the resonance frequency of a given mode of the plate. For this reason, the finger acoustic force does not represent the totality of the contact force, but the component measured at the resonance frequency of the plate.

2.2 Modelling in the rotating reference frame

For obtaining $\tilde{f}_r$, it is necessary to solve equation (5) in the time domain, by measuring the variables $w(t)$ and$v(t)$. These are, however, high frequency signals, which are hard to manage on a portable device. This means that $\tilde{f}_r$ can only be acquired at the expense of a high sampling rate, and off-line calculations. In order to address this issue, the time domain equations can be transformed into a rotating reference frame.

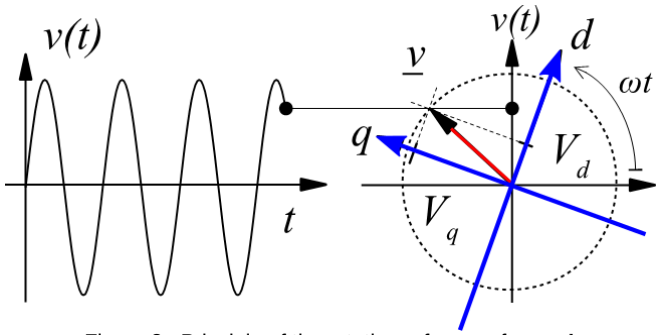

Figure 2. Principle of the rotating reference frame dq.

Assuming that $v(t)$ is a sinusoidal function, it can be represented by the use of complex phasors, as in equation (5), where $\underline{v}$ is the phasor of v such that $v(t)$ is the imaginary part of $\underline{v}$.

$$\underline{v}(t) = (V_d + jV_q)e^{j\omega t} \qquad (8)$$

V_d and V_q are the coordinates of $\underline{v}$ in the rotating reference frame dq. This representation is illustrated in figure 2.

In the same way, we define W_d, W_q, F_{rd} and F_{rq}.

The method for imposing V_d and V_q in order to control W_d and W_q is detailed in [1]

In the remaining of this paper, the plate is controlled in such a way that $W_q = 0$, leading to $\underline{\dot{w}} = j\omega W_d e^{j\omega t}$. Equation (5) leads to two new equations, after projecting on axis d and q:

$$\tilde{F}_{rd} = NV_d \quad , \qquad \tilde{F}_{rq} = NV_q - D\omega W_d \qquad (9)$$

2.3 Theoretical examples

For the purpose of illustration, we present three examples of an acoustical finger force observation. In the first example, we consider a no load condition (the probing finger is absent), leading to $f_r = 0$. Then, the equation (9) yields:

$$V_d = 0 \qquad V_q = \frac{D}{N}\omega W_d \qquad (10)$$

Hence, at no load, V_q is proportional to W_d, and the slope is $DN\omega$; this property is exploited later, in order to calibrate the measurements.

In the second example, the finger is always in contact with the vibrating plate. So the contact force is assumed to be sinusoidal in steady state. Due to the acoustical impedance of the finger pulp, the contact force depends on the vibration itself. If we consider a typical model that includes the internal damping of the skin (denoted by D_f) and the vibrating mass M_f [4], the acoustical finger force is sinusoidal, and can be writtenthanks to the fundamental mechanical law: $f_r = D_f\dot{w} + M_f\ddot{w}$, leading to:

$$F_{rd} = -M_f\omega^2 W_d \qquad F_{rq} = D_f\omega W_d \qquad (11)$$

The acoustical force is then shared between the axes: the d axis contains the inertial force while the q axis contains the damping force.

In the last example, we consider intermittent contact induced by an ideal elastic shock. When the contact is intermittent, f_r consists of pulses at the frequency of the vibration (as illustrated in Figure 3), and with a phase shift named $\emptyset$ [3], [5]. Each time the skin bounces on the plate, the force f_r increases before returning to 0 when the skin is detaching from the plate. For illustrative purpose, we consider a perfect rebound of the skin: the contact time equals zero, and the contact force is infinite when the plate touches the finger. Therefore, we write f_r as a Dirac comb distributionwith $f_r = f_0 \sum_{n=-\infty}^{\infty} \delta\left(t - \frac{2\pi n - \Phi}{\omega}\right)$. It should be emphasized here that the average of f_r is f_0 by definition of the delta function. It is also the normal force F_N, divided by the pulse period. Hence, the mean value of F_N over k pariods can be expressed as (12).

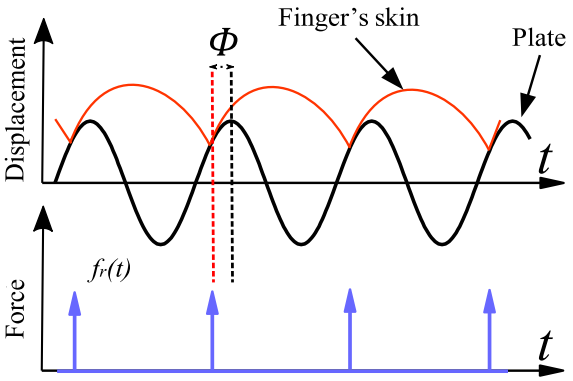

Figure 3. Evolution of f_r in case of an ideal intermittent contact. Angle Φ represents the phase between the displacement peak and the force peak.

$$F_N = \frac{1}{kT} f_0 \sum_{n=-\infty}^{\infty} \int_T \delta\left(t - n\frac{2\pi - \Phi}{\omega}\right) dt$$

$$= f_0\, {}^{k}/_{kT} \quad \text{so,} \qquad (12)$$

$$f_0 = F_N T$$

The acoustical finger force f_r contains a fundamental, which is at the resonance pulsation of the plate, and harmonics. Due to the resonant behavior of the plate, the harmonics do not influence the plate's vibration, and therefore, only the fundamental can be observed with equation (11). In the particular case of ideal intermittent contact condition, he forces F_{rd} and F_{rq} are then calculated by 1st harmonic decomposition. For example, considering F_{rd} in (13)

$$F_{rd} = 2\left(\frac{\omega}{2\pi}\right) \int_{\left(\frac{2\pi}{\omega}\right)} f_r(t)\cos(\omega t)dt$$

$$= 2\left(\frac{\omega}{2\pi}\right) f_0 \sum_{n=-\infty}^{\infty} \int_{\left(\frac{2\pi}{\omega}\right)} \delta\left(t - \frac{2\pi n - \Phi}{\omega}\right)\cos(\omega t)dt \qquad (13)$$

$$F_{rd} = 2\left(\frac{\omega}{2\pi}\right) \int_{\left(\frac{2\pi}{\omega}\right)} f_r(t)\cos(\omega t)dt$$

$$F_{rd} = 2\left(\frac{\omega}{2\pi}\right) f_0 \cos(\Phi) = 2\left(\frac{\omega T}{2\pi}\right) F_N \cos(\Phi)$$

The same procedure can be performed for F_{rq}, using $\sin(\Phi)$. If intermittent contact occurs at every period (like illustrated in figure 2), then $T = {}^{2\pi}/_{\omega}$. Hence, when the contact is intermittent, F_{rd} and F_{rq} can simply be represented by (14) (if on the other hand, a sub-harmonic occurs, $T = 4, 6, 8, \ldots\ {}^{\pi}/_{\omega}$ and F_{rd} will be calculated over 1, 2, 3, … periods and the result is the same).

$$F_{rd} = 2F_N \cos(\Phi) \qquad F_{rd} = 2F_N \sin(\Phi) \qquad (14)$$

From this result, it can be inferred that, with the type of contact proposed in the third example, the observation of the acoustical finger force is not related to the acoustical impedance of the finger pulp, and the components along

the axis d and q are not related to a damping or a mass. However, the phase shift, which can be calculated from $tan^{-1}\left(\frac{\bar{F}_{rq}}{\bar{F}_{rd}}\right)$ is related to the time at which the contact occurs.

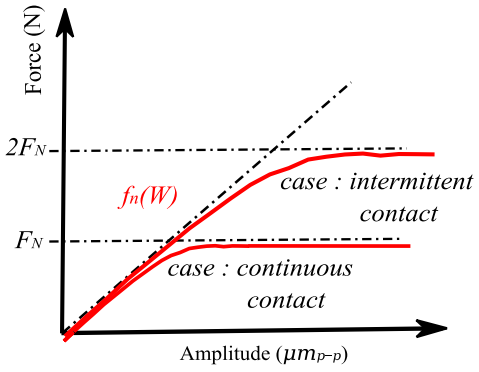

Figure 4. Theoretical evolution of of $f_r(W)$ when intermittent contact is achieved, or not, according to example models

Over an amplitude sweep, it is possible that the conditions for examples 2 and 3 occur consecutively. That is, for lower amplitudes the finger remains in contact with the plate, and the forces in the dq frame are defined by (11). From a given amplitude (hereby defined *'breakpoint'*), intermittent contact occurs, and thus the forces would be defined by (14). In this case, the theoretical evolution of f_r would describe an initial linear section, followed by a saturation at a maximum value $f_r = 2F_N$.

Alternatively, it could happen that the finger does not 'bounce'. In that case, the saturation is expected at F_N.

Both cases are illustrated in Figure 4.

3 Experimental Setup and Protocol

3.1 Material

The setup for this experiment is as shown in Figure 5. An aluminum beam ($18\ x\ 119\ x\ 2$ mm^3) is covered with a hydrophobic surface, and sustained by a structure equipped with a 6-dimensional force sensor (ATI Nano 43); an analog Standard Volume Indicator (SVI) gives an indication of the pressing force. Four piezoelectric ceramics of dimensions ($16\ x\ 4\ x\ 0.5$ mm^3) are glued to the opposite surface of the beam to produce the vibration. One of them is used as a vibration amplitude sensor. The positioning of this sensor has been chosen to coincide with a maximum of deformation, according to the modal shape $\Psi(x, y)$, thus maximizing the measurement of f_r via relation (6) at any vibration amplitude.

The geometry of the beam, size and position of the piezoelectric ceramics are designed and simulated with a FE analysis in order to obtain a pre-defined normal wave vibration mode at the plate's resonance frequency. We obtained a resonant frequency of 24870 Hz. Closed loop control of the vibration amplitude of the beam is achieved thanks to the use of a Digital Signal Processor (STM32F4 from ST Microelectronics). The acoustical forces are observed online, and sent to a main computer through a serial connection for data collection. The vibration control is achieved at 10 kHz. An external power amplifier (HSA 4051 from NF, Japan) amplifies the controller's output up to 300 V peak-peak.

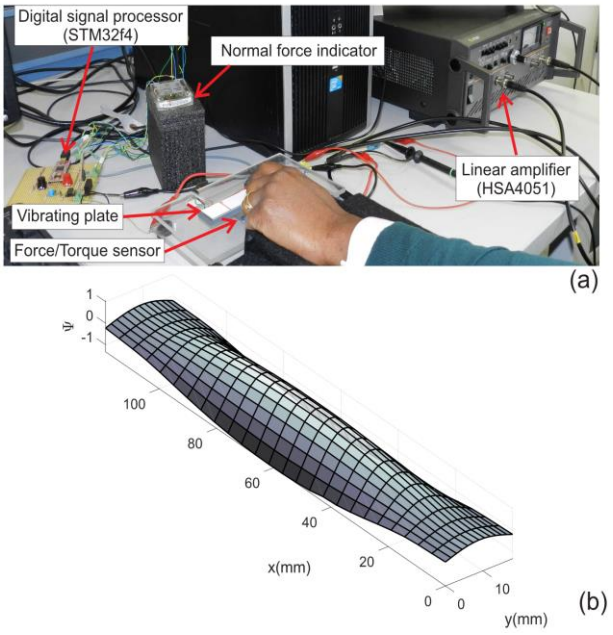

Figure 5. The experimental setup; (a) is the general view and (b) is the plate deformation mode shape $\Psi(x, y)$.

The parameter N of the plate has been identified using the methodology described in [11] and its value is N= 0.02NV^{-1}. The no-load test measurement has been used to identify D=0.2848 Nsm^{-1}, from (10), with an amplitude sweep W_d varying back and forth from 0 to $2\mu m_{p-p}$ (with 20 steps of $0.1\mu m_{p-p}$), $V_d = 0$ and $V_q = 12\text{x}10^6 W_d$.

3.2 Experimental procedure

Twelve healthy perople aged from 22 to 60 participated to the experiments. They were asked to thoroughly wash and dry their hands before the tests. All participants gave written informed consent. The investigation conformed to the principles of the Declaration of Helsinki and experiments were performed in accordance with relevant guidelines and regulations.

Prior to any experiment, the participants trained themselves to apply a constant pressure of 0.4 N onto the plate for some seconds, by following the indication of the SVI.

Two experiments were designed in this work. In the first experiment, the participants placed their finger on the middle of the plate, standstill, with an angle of 45°, pushing with a normal force of 0.4 N. During the experiment, the vibration amplitude W_d is imposed in close loop control, just as for the no-load condition, i.e. W_d varying back and forth from 0 to $2\mu m_{p-p}$ (with 20 steps of $0.1\mu m_{p-p}$). The cycle is repeated five times. The components F_{rd} and F_{rq} are recorded at the end of each step.

In the second experiment, the participants moved their finger laterally from left to right, along the surface of the plate. They were asked to keep an inclination of 45° and a

pressing force of 0.4 N. To control the finger's speed, a metronome emits sound at 1bps and participants are asked to move their finger between two lines marked on the plate during two metronome clicks. The nominal speed is then equal to 70 mms^{-1}. During this try, the sinusoidal vibration amplitude applied to the plate is modulated by a 5 Hz square signal varying from 0 to to $2\mu m_{p-p}$, and the normal and tangential forces are recorded at a sampling rate of 100 Hz.

The second experiment is performed right after the first one, keeping the same experimental conditions, to benefit from the training of the finger inclination and pressing force, as well as to keep the participant's skin in the same condition. Actually, it was observed during the tests, that the participants controlled the pressing force with a higher pressure than required (average=0.515N), but maintained it almost constant over the test (standard deviation SD=0.07N over all participants).

4 RESULTS

4.1. Result from experiment 1

In Figure 6 the measurements of acoustic force, $\tilde{F}_{rd}$ and $\tilde{F}_{rq}$ and their average acoustic force magnitude $\tilde{F}_r = \left(\sqrt{F_{rd}^2 + F_{rq}^2}\right)$ are depicted for all participants.

We notice that the evolution and maximal values of the observed $\tilde{F}_r$ and components $\tilde{F}_{rd}$ and $\tilde{F}_{rq}$ differ from one participant to another, due to the different mechanical properties of the skin of every participant.

The theoretical values from the examples illustrated in Figure 4 section 2.3., for an applied pressure of about 0.5N, led to expect a lineary increasing $\tilde{F}_r$, with a saturation occurring at about 1N. However, the actual measurements exhibit a different behavior for most participants. Some subjects, such as 1-2, and 8-12, provide a measurement up to two times higher than the expected 1N. Others, such as 4, 6 and 7 seem to reach a lower inflection point (or 'breakpoint), at about 0.5N, but steadily increase from there. This result leads to the conclusion that the intermittent contact models used for the examples are perhaps lacking a few elements to describe the full complexity of the contact between the finger and the plate.

A possible explanation for this difference may be related to the non-consderation of the existing column of air between the finger and the plate when there is contact loss (the reason for the squeeze film effect). This phenomenon could, for example, explain why some participants reach larger $\tilde{F}_r$ than the theoretical saturation value of 1N. This could be the case if, for example, f_r took negative values for a portion of the vibration period, due to negative pressures or 'suction' forces during the loss of contact.

4.2. Result from experiment 2

The results of the second experiment helped to characterize the friction modulation for each participant. Figure 7 depicts a typical friction measurement when the participant is sliding her/his finger over the tactile plate. A positive friction coefficient (denoted μ) is obtained when the

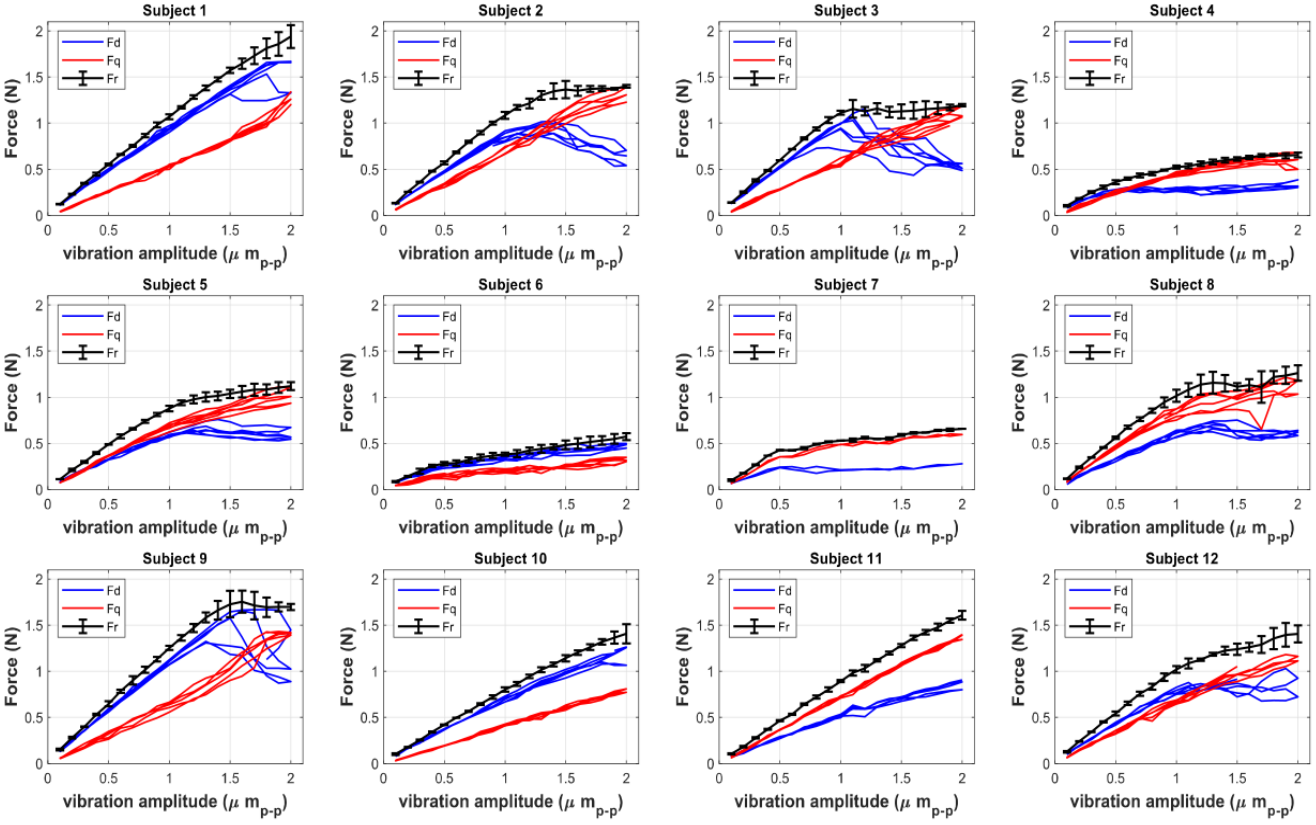

Figure 6. Measured force values $\tilde{\mathbf{F}}_{\mathbf{rd}}$ (red), $\tilde{\mathbf{F}}_{\mathbf{rq}}$ (blue) and the force magnitude $\tilde{\mathbf{F}}_{\mathbf{r}}$ (black), as a function of **W** for every participant

finger is sliding from left to right, while a negative μ is obtained in the reverse direction. The modulation of μ is due to the modulation of the vibrating amplitude W (with the 5 Hz square signal) while sliding.

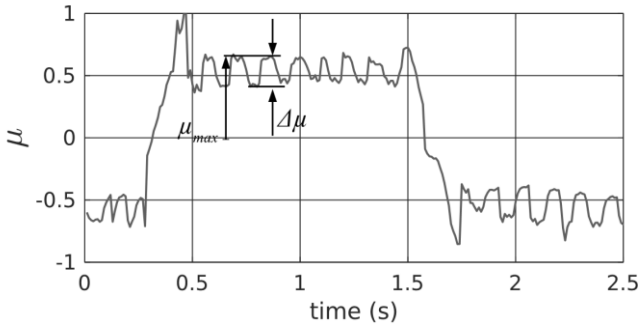

Figure 7. Typical friction coefficient μ as a function of time for one participant

To characterize the friction modulation, we calculate for each participant the maximum of μ, named μ_{max} and the friction reduction denoted $\Delta\mu$. Since the value may change from one period of the modulating signal to another, we average the measurement over 6 periods of friction modulation (considering either the positive or negative coefficients).

The obtained values are represented in the bar graph in Figure 8. It is possible to observe that the friction coefficient and its variation may be very different from one participant to another. Some measurements, such as those for subjects 3 -7, have a low μ_{max} (below 0.5). It can be verified from Figure 6 , that these participants also have a low value of maximal acoustical finger force (less than 1.6 N). Participants of the other group, 1-2, 8-12, have a high level of friction (above 0.5) and a minimum force of 1.5 N. Therefore, it seems reasonable to consider a correlation between the acoustical force measurement, and the level of friction with and without ultrasonic vibration.

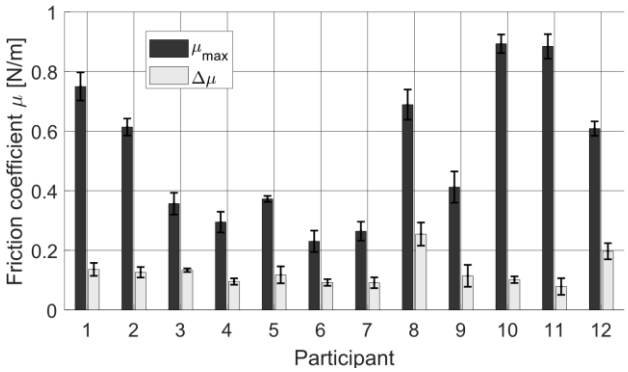

Figure 8. Maximum of friction μ_{max} and $\Delta\mu$ for each participant

5 PCA OF THE FINGER ACOUSTIC FORCE MEASUREMENT AND ITS CORRELATION WITH FRICTION

In order to elucidate a possible relation between the fundamental acoustical force calculation and the friction coefficient between the finger and the plate (and how it changes due to vibration), two hypotheses are analysed. Firstly, it is necessary to determine, whether the mean acoustic force magnitude of a given participant 'p', $\widetilde{F}_{rp}$, can be expressed as a separable function of two distinct factors. The first factor is related to the motion of the plate, i.e. a function of the vibration amplitude, which will be denoted $f(W)$. The second factor is specific to the mechanical properties of the participant's finger i.e. a function of each subject, which will be denoted $\sigma(p)$. If the two effects are separable, $\widetilde{F}_{rp}$ could be decomposed into the addition of 'n' response types (similar to a modal decomposition), to be expressed as in equation (15). A PCA would therefore be useful for building such a model.

$$\widetilde{F}_{rp} = \sum_{n=1}^{\infty} f_n(W)\sigma_n(p) \qquad (15)$$

The second hypothesis deals with a possible relation between the acoustic force response and the friction between the finger and the plate (and how this friction reduces when the plate vibrates). If it is indeed possible to find a model for the acoustic force response, where a few participant's parameters are differenciated from the influence of the vibration amplitude, it could then be possible to find if there is a relation between these parameters and the friction of the finger with and without vibration. This second hypothesis suggests as well that the possible influence of an additional factor (not plate or finger, but for example, air) in this relation is neglectible.

If these two hypotheses are validated, it would mean that the friction between the finger and the plate, with and without vibration, may be inferred with a certain precision, by measuring the finger's acoustic force response. Moreover, if equation (15) is validated, this may help identify the influence of the human factor in the force response. Such a result may serve to identify certain finger parameters in an improved analytical model similar to the one exemplified in section 2.

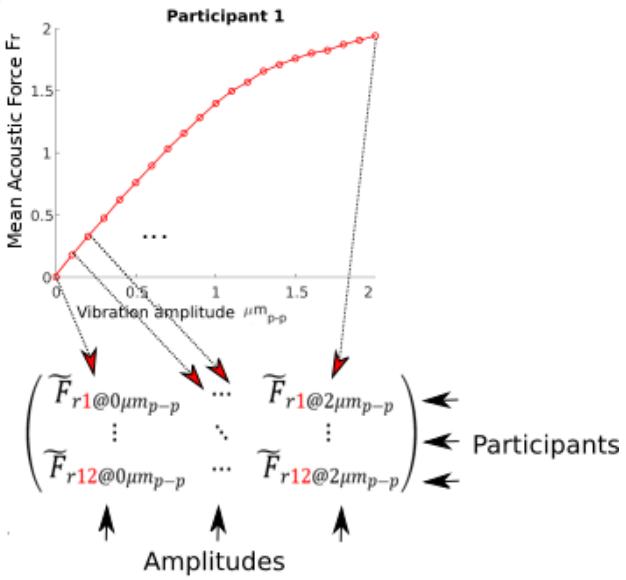

Figure 9. Construction of matrix FR from the participant's mean acoustic force calculation

For analyzing the first hypothesis, one acoustic force matrix FR is constructed as shown in Figure 109. Each element of FR corresponds to the mean acoustic force magnitude $\widetilde{F_r}$ calculation from the measurements at each vibration amplitude (20 scanned amplitudes from 0 to $2\mu m_{p-p}$), for each participant (12 subjects). FR has, therefore, a dimension of 20x12, where the rows represent any given participant, and the columns a vibration amplitude.

A PCA analysis is made for FR. The PCA helps represent the data as a series of projections on subsequent orthogonal normalized axes which will maximize the variance amongst datapoints. These axes are called 'components'. The first component corresponds to the direction which explains the highest percentage of the variance while the succeeding ones explain the rest of the percentage of the variance in decreasing order.

The components which are able to represent most of the variance between data points are denominated 'principal' components (e.g. for a given data set, principal component 1 (PC1) could explain 90% of the variance, PC2 5%, PC3 0.5%, and so on). The PCA helps re-writing matrix FR as shown in equation (15), where Sc_n represent the percentage of the variance explained by each component.

$$\begin{pmatrix} \tilde{F}_{r1@0\mu m} & \cdots & \tilde{F}_{r1@2\mu m} \\ \vdots & \ddots & \vdots \\ \tilde{F}_{r12@0\mu m} & \cdots & \tilde{F}_{r12@2\mu m} \end{pmatrix} = \begin{pmatrix} f_1(0\mu m) \\ \vdots \\ f_1(2\mu m) \end{pmatrix} \begin{pmatrix} \sigma_1(p_1) & 0 & \cdots & 0 \\ 0 & \sigma_1(p_2) & 0 & \vdots \\ \vdots & \vdots & \ddots & \vdots \\ 0 & 0 & \cdots & \sigma_1(p_{12}) \end{pmatrix} Sc_1 + \begin{pmatrix} f_2(0\mu m) \\ \vdots \\ f_2(2\mu m) \end{pmatrix} \begin{pmatrix} \sigma_2(p_1) & 0 & \cdots & 0 \\ 0 & \sigma_2(p_2) & 0 & \vdots \\ \vdots & \vdots & \ddots & \vdots \\ 0 & 0 & \cdots & \sigma_2(p_{12}) \end{pmatrix} Sc_2 + \cdots \quad (16)$$

A single significant PC in the analysis can be interpreted as a correlation between the measured data, explainable by a simple linear combination of the measurements. In other words, if the score for PC1, Sc_1, is large enough (larger than 95%, for example), the mean acoustical force magnitude response for every participant could be represented by more or less the same 'shape' $f_1(W)$ (which is constructed by combining the results of every participant), multiplied by a constant for each participant $\sigma_1(p)$.

5.1. PCA results for FR

After doing the analysis, it was found that PC1 explains over 97% of the variance of the data in matrix FR. In other words, in the 12-dimensional space created by the measurements of each participant at each vibration amplitude, there exists a one-dimensional sub-space (a single axis: PC1), which serves to accurately represent most of the variance of the data (it can be seen that the variation in PC2 is much smaller in comparison to the variation in PC1). Figure 10 represents the biplot of the force data (red dots) in the PC1, PC2 plane. In blue, each axis represents the projection of each participant on the principal component plane. If it was desired, for example, to find the value of the data for one of the 12 participants, it would suffice to project the point into the axis corresponding to the desired subject. For this reason, axes which are projected close to each other are expected to produce similar $\widetilde{F_r}$ responses.

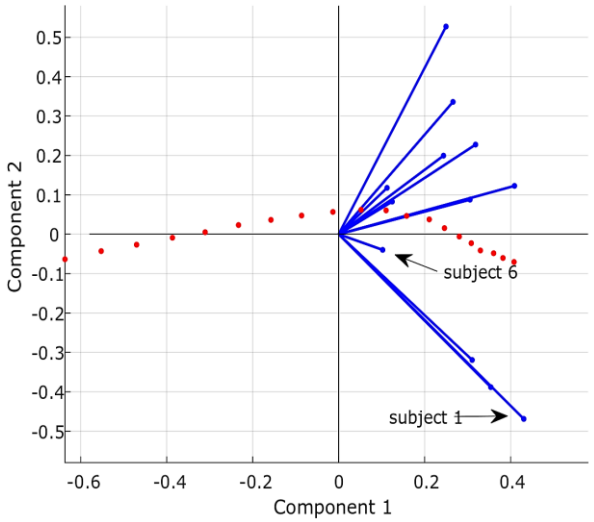

Figure 10. Biplot of $\widetilde{F_r}$ data from 0 to $2\mu m_{p-p}$ in PC1, PC2 plane. In blue, the projectios of the axes of each participant in the PC plane

This result confirms hypothesis 1, that the function describing $\widetilde{F_{rp}}$ at a given amplitude can be represented by separating the influence of the plate from the one of the human. Hence, (15) could be simplified to (15) if only one PC is considered, and to (15) if we consider PC1 and PC2.

$$\widetilde{F}_{rp} = f_1(W)\sigma_1(p) \quad (17)$$

$$\widetilde{F}_{rp} = 0.97 f_1(W)\sigma_1(p) + 0.03 f_2(W)\sigma_2(p) \quad (18)$$

Thanks to this result, the sought human characteristic becomes simpler to find. If (15) is considered, for a given participant p, $\sigma_1(p)$, can be estimated from the knowledge of $f_1(W)$, and the measurement of $\widetilde{F_{rp}}$. Moreover, given that $f_1(W)$ is already known, $\sigma_1(p)$ can be estimated by measuring a single data point at a given amplitude for subject p. If two PC were considered, as in (18), two datapoints would serve to find $\sigma_1(p)$ and $\sigma_2(p)$, and so on. For this reason, it can be assumed that force data extrapolation is feasible. Consequently, if an additional person p_{13} is included, their complete acoustical force response can be reconstructed from a single point (or two) measurement of $\widetilde{F_{rp}}$.

5.2. Coefficient σ_1 estimation and $\widetilde{F_{rp}}$ extrapolation from a single measurement, considering only one PC

A reconstruction of a person's force response from one point and the PCA data is illustrated in an example.

Here, participant 12 ($\sigma_1(p_{12}) = 0.305$) is removed from the calculation. A PCA is then performed with 11 participants. One measurement of the 12th subject is taken. For this example, the mean force magnitude at $2\mu m_{p-p}$ vibration is measured ($\tilde{F}_{r12@2\mu m} = 1.406N$). The estimated coefficient of the 12th subject can thus be calculated by dividing the measured data point, by the value contained in the principal component at the same amplitude of $2\mu m_{p-p}$: $\sigma_{1_{est}}(p_{12}) = \tilde{F}_{r12@2\mu m}/f_1(2\mu m_{p-p})$. This coefficient $\sigma_{1_{est}}(p_{12}) = 0.311$, is then used to re-calculate the force response for subject 12 at each point, as can be seen in Figure 11. The estimation is compared to the measurement for subject 12 on this figure.

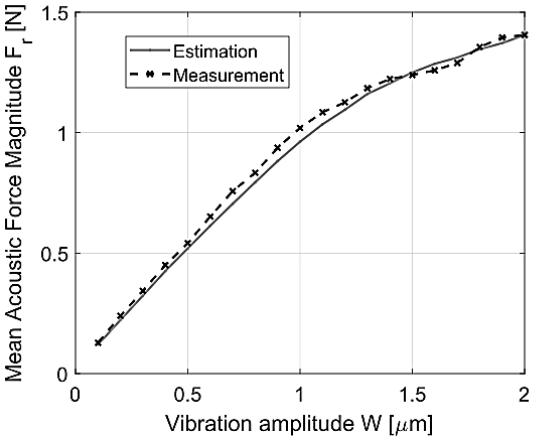

Figure 11. Estimation of the force response from one force measurement using the PCA model with only one principal component

The results show a fairly accurate estimation of $\widetilde{F_r}$ for participant 12 at each amplitude, with a mean relative error of about 1.5% and a maximum relative error of less than 8% at each point.

In order to confirm that PC1 provides a good enough representation of the data for the tested population, an estimated $\sigma_{1_{est}}(p)$ can be made for each subject in the trial, by using the same method explained in the example (performing the PCA for 11 participants and estimating the datapoints of the remaining one from a single measurement). This value is compared to the actual coefficient $\sigma_1(p)$ derived from the PCA with the actual data.

The results of the coefficient estimation are listed in table 1. The average relative error for all meaursments is less than 8%, with the largest being about 30%.

Overall, it can be concluded that the model obtained from the PC1 is accurate enough to predict $\sigma_1(p)$ of most participants with a single measurement, with certain exceptions such as such as subjects 4, 6 and 7, for whom the error is still rather significant.

Albeit the fairly accurate estimation of $\sigma_1(p)$, it is possible that the use of a single PC may hinder the precision of the complete force response extrapolation for some participants.

TABLE 1
COEFFICIENT DERIVED FROM PCA VS. ESTIMATED COEFFICIENT FROM A SINGLE DATAPOINT

p	σ_1	σ_{1est}	err1%
1	0.431	0.428	0.72
2	0.318	0.308	3.23
3	0.250	0.265	6.01
4	0.124	0.145	16.39
5	0.244	0.247	1.45
6	0.102	0.127	23.99
7	0.113	0.145	29.24
8	0.266	0.280	5.23
9	0.409	0.368	9.93
10	0.311	0.311	0.01
11	0.354	0.355	0.29
12	0.305	0.311	1.75

To improve this potential issue, equation (13) can be considered, and an additional component, PC2, may be added to the model.

This new result, will allow evaluating if the estimation is improved by measuring two points instead of one.

5.3. Coefficients σ_1 and σ_2 estimation and $\widetilde{F_{rp}}$ extrapolation from a two-point measurement

A similar approach to section 5.2. is considered. However, two points are now measured: $P_1 = \tilde{F}_{rp@2\mu m}$ and $P_2 = \tilde{F}_{rp@1\mu m}$. Knowing these two points, the new $\sigma_1(p)$ and $\sigma_2(p)$ can be estimated as from equations (19) and (20).

$$P_1 = 0.97 f_1(2\mu m_{p-p})\sigma_1(p) + 0.03 f_2(2\mu m_{p-p})\sigma_2(p) \quad (19)$$

$$P_2 = 0.97 f_1(1\mu m_{p-p})\sigma_1(p) + 0.03 f_2(1\mu m_{p-p})\sigma_2(p) \quad (20)$$

The result of the estimation of $\sigma_1(p)$ and $\sigma_2(p)$ are listed in table 2, with their corresponding relative error.

If the results on table 2 are compared to those on table 1, it can be noticed that the coefficient estimation is not significantly improved by the inclusion of a second component. However, the comparison of the estimation of the complete data for each participant, which is presented in figure 12, leads to a different conclusion.

In this figure it can be noticed how, for many of the participants, PC1 seems to provide a fair approximation of their force response. Nevertheless, an important improvement of the approximation for all subjects is achieved thanks to the use of a second component (measurement errors may justify the inaccuracies).

5.4. Friction correlation with PCA results from a single point measurement (one PC)

Moving on to the second hypothesis, we wish to determine whether a relation can be found between the data recovered from the PCA of the measurements and the friction coefficient of the finger against the plate.

TABLE 2
COEFFICIENTS DERIVED FROM PCA VS. ESTIMATED COEFFICIENT FROM TWO DATAPOINTS

p	σ_1	σ_2	σ_{1est}	σ_{2est}	err1%	err2%
1	0.431	-0.469	0.435	-0.497	1.1	6.0
2	0.318	0.228	0.303	0.219	4.8	3.6
3	0.250	0.527	0.262	0.535	5.0	1.4
4	0.124	0.083	0.143	0.133	14.9	60.8
5	0.244	0.199	0.244	0.197	0.1	1.5
6	0.102	-0.040	0.127	-0.024	23.9	40.8
7	0.113	0.118	0.144	0.143	27.8	21.6
8	0.266	0.336	0.277	0.255	4.1	24.2
9	0.409	0.123	0.364	0.162	11.0	32.2
10	0.311	-0.319	0.314	-0.296	1.1	7.3
11	0.354	-0.388	0.361	-0.392	2.0	0.8
12	0.305	0.088	0.309	0.097	1.0	10.6

Firstly, in figure 13, the estimated coefficients $\sigma_{1_{est}}(p)$ are plotted against the friction coefficient μ_{max} without vibration, μ_{min} when there is vibration at $2\mu m_{p-p}$, and finally against the relative friction coefficient reduction $\Delta\mu/\mu_{max}$ (a parameter associated with perception).

Linear regressions between $\sigma_{1_{est}}$ and μ_{max}, μ_{min} and $\Delta\mu/\mu_{max}$ are calculated. The resulting relations are expressed in (21) - (23).

$$\mu_{max} = 1.9\sigma_{1_{est}}(p) + 0.015 \quad (21)$$

$$\mu_{min} = 1.8\sigma_{1_{est}}(p) - 0.078 \quad (22)$$

$$\Delta\mu/\mu_{max} = -0.72\sigma_1(p) + 0.47 \quad (23)$$

TABLE 3
FRICTION COEFFICIENT MEASUREMENT VS. ESTIMATION FROM PCA COEFFICIENTS AND LINEAR REGRESSION

p	μ_{max}	μ_{min}	$\mu_{max_{est}}$	$\mu_{min_{est}}$	err1%	err2%
1	0.750	0.614	0.827	0.692	10.3	12.7
2	0.614	0.487	0.600	0.477	2.2	2.2
3	0.357	0.224	0.518	0.398	45.1	78.1
4	0.295	0.200	0.290	0.183	1.6	8.4
5	0.373	0.255	0.485	0.367	30.1	44.1
6	0.230	0.138	0.256	0.150	11.1	8.8
7	0.264	0.173	0.291	0.184	10.2	6.3
8	0.689	0.434	0.547	0.426	20.7	2.0
9	0.412	0.298	0.715	0.585	73.4	96.7
10	0.893	0.792	0.605	0.481	32.3	39.3
11	0.884	0.806	0.689	0.561	22.1	30.4
12	0.609	0.411	0.606	0.481	0.5	17.0

When performing the approximation, we find that that μ_{max} has a correlation of about 75% with the estimated $\sigma_1(p)$ and a standard mean squared error of 0.53. For μ_{min} we get a correlation of about 71% and a standard mean squared error of 0.54. In the case of friction contrast, the relation between $\sigma_{1_{est}}(p)$ has a smaller correlation of about 65% a standard mean squared error of 0.26.

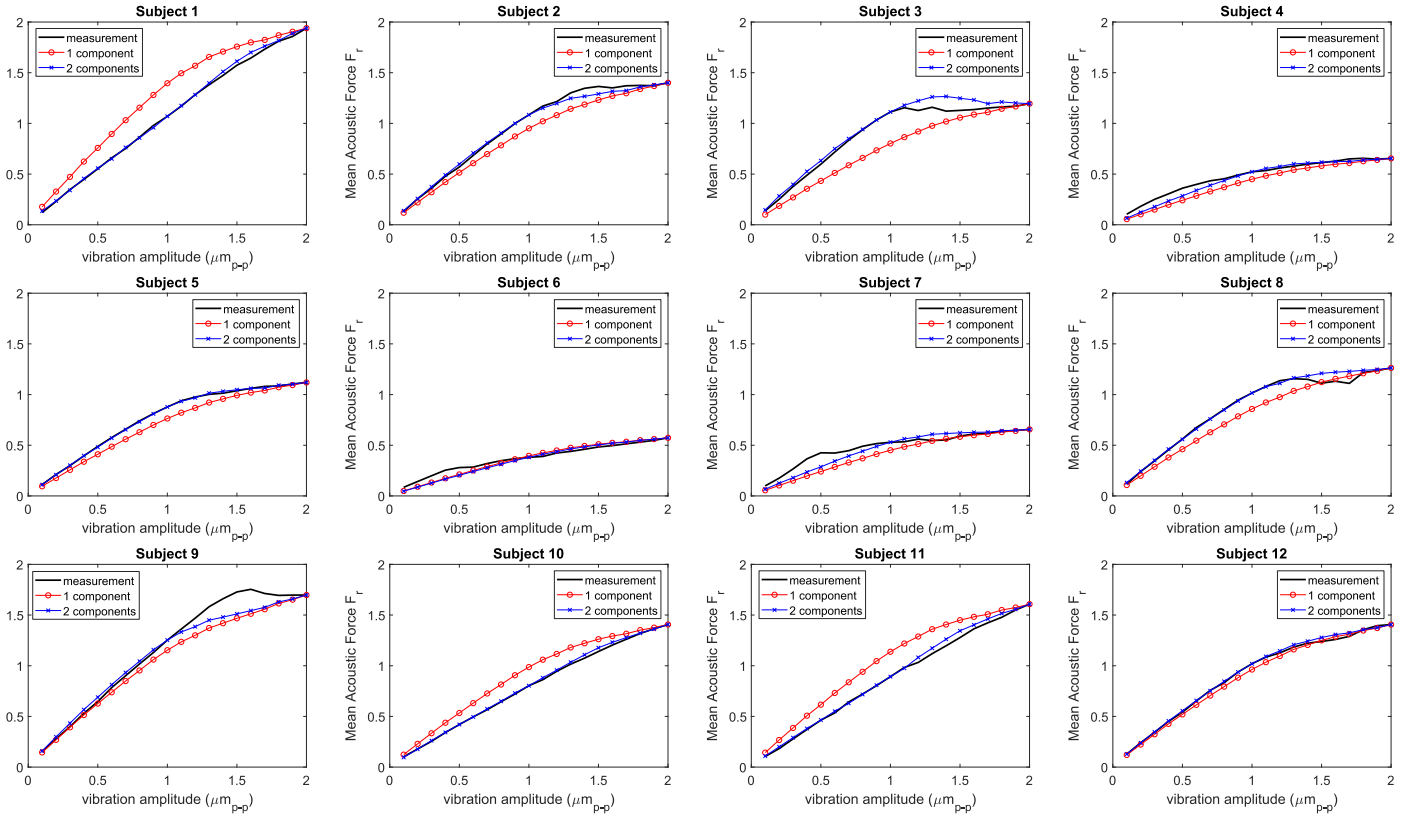

Figure 12. Mean Acoustical Force estimation comparison: using one PC (red), and using two PC (blue)

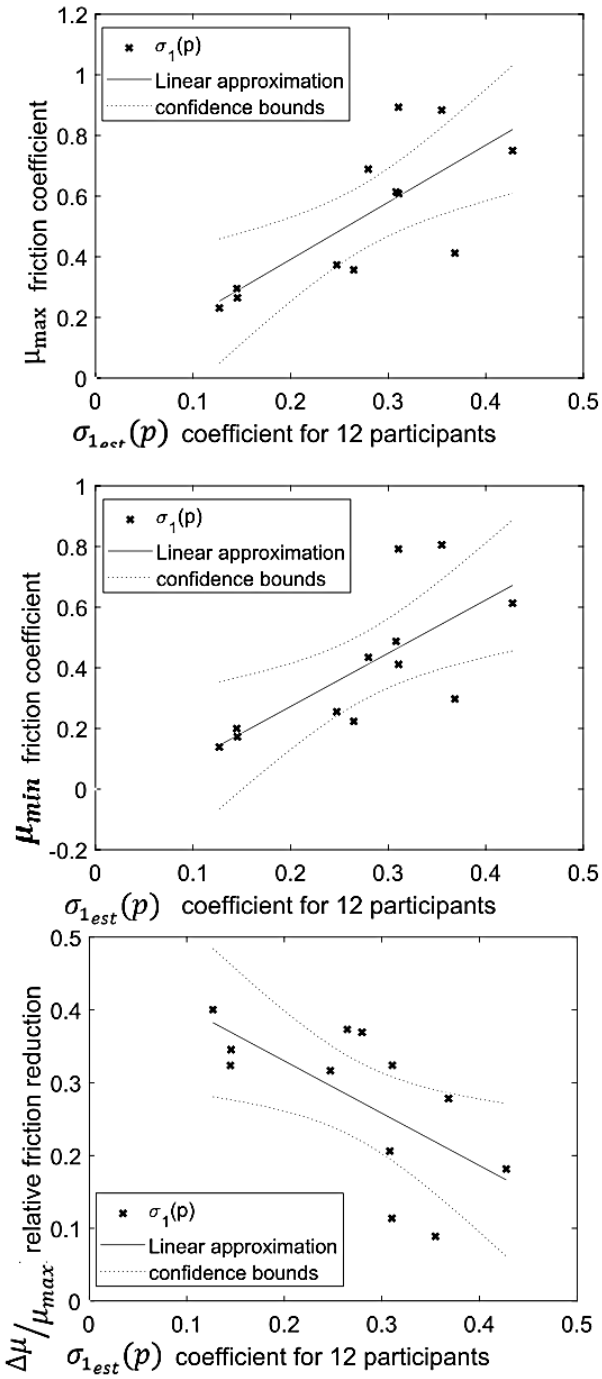

Figure 13. Relation between participant data from PCA $\sigma_1(p)$ and (up) friction coefficient without vibration, (center) friction coefficient with $2\mu m_{p\text{-}p}$ vibration, (down) relative friction reduction.

The friction coefficients are estimated with the linear regressions given by (21) - (21) (which give the highest correlation) for each participant. Table 3 details the estimation and relative error of the μ_{max} and μ_{min} estimations (using $\sigma_{1_{est}}$), against the corresponding measurements.

The approximation is fair, with an average error of about 22% for μ_{max} and 28% for μ_{min}, eventhough a group ofoutliers are identified. This result might be improved by the inclusion of PC2 to the analysis.

5.5. Friction correlation with PCA results from a two-point measurement (PC1 and PC2)

With the inclusion of a second datapoint measurement, the friction coefficient with or without vibration (μ) may be expressed as in (24).

$$\mu = A\sigma_{1_{est}}(p) + B\sigma_{2_{est}}(p) + C \qquad (24)$$

Given that coefficients 'A', 'B' and 'C' in (19) are unknown, an optimization is carried out, in order to maximize the correlation of the left and right side of (19) for $\mu = \mu_{max}$, $\mu = \mu_{min}$ and $\mu = \Delta\mu/\mu_{max}$. The algorithm produces relations (20) – (22).

$$\mu_{max} = 1.97\sigma_{1_{est}}(p) - 0.36\sigma_{2_{est}}(p) + 0.03 \qquad (25)$$

$$\mu_{min} = 1.37\sigma_{1_{est}}(p) - 0.28\sigma_{2_{est}}(p) + 0.02 \qquad (26)$$

$$\Delta\mu/\mu_{max} = -0.32\sigma_{1_{est}}(p) + 0.17\sigma_{2_{est}}(p) + 0.37 \qquad (27)$$

The correlation between the caculations and the measured values is 83%, 85% and 83% for μ_{max}, μ_{min} and $\Delta\mu/\mu_{max}$ respectively.

The friction coefficients are estimated with the linear regressions given by (21) - (21) (which give the highest correlation) for each participant. Table 3 details the estimation and relative error of the μ_{max}, μ_{min} and $\Delta\mu/\mu_{max}$ estimations (using $\sigma_{1_{est}}$ and $\sigma_{2_{est}}$), against the corresponding measurements.

TABLE 3
FRICTION COEFFICIENT MEASUREMENT VS. ESTIMATION FROM PCA COEFFICIENTS AND LINEAR REGRESSION

p	$\mu_{max_{est}}$	$\mu_{min_{est}}$	$\frac{\Delta\mu}{\mu_{max_{est}}}$	err1%	err2%	Err3%
1	1,1	0.75	0.14	42.6	22.8	20.1
2	0.55	0.37	0.31	10.2	24.2	49.1
3	0.36	0.22	0.37	0.0	0.0	0.0
4	0.27	0.17	0.34	9.8	12.5	6.3
5	0.44	0.29	0.32	18.8	15.7	1.9
6	0.29	0.20	0.32	26.1	42.5	19.3
7	0.26	0.17	0.35	0.0	0.0	0.0
8	0.49	0.32	0.32	29.4	25.6	13.0
9	0.69	0.47	0.28	67.7	57.5	0.0
10	0.76	0.53	0.22	15.2	33.0	91.2
11	0.88	0.62	0.19	0.0	22.8	109.7
12	0.61	0.41	0.29	0.5	0.0	12.0

The correlation and error are improved by including a new component in the approximation. Nonetheless, some error margin remains. This may be due to measurement error, or perhaps a missing parameter in the relation.

7 DISCUSSION

The measurement of the fundamental acoustical finger force has been achieved on a portable device, with the help of a Digital Signal Processor, and does not require off line calculation. We obtained measurements from 12 participants, which are plotted in Figure 6. From the observations, it can be noted that for most participants, the force response in function of the vibration amplitude increases

linearly up until a given amplitude (hereby named 'breakpoint'), when either the d or the q (or both) axes saturate, and the response is non-linear. We believe that this change in force behavior corresponds to the onset of the intermittent contact. This inflection point is different from one participant to another. This might be due to the different mechanical skin parameters. Indeed, it has been shown that intermittent contact occurs for higher vibration amplitude for soft skin [3].

One may notice that the behavior of the calculated mean acoustic force differs in magnitude as the expectations which can be made from the examples provided in section 2. In the case of ideal intermittent contact producing pulsed forces as depicted in Figure 3, the fundamental of the acoustical finger force is expected to measure maximum two times the mean value of the pressing force (0.4 – 0.5N). A few explanations may be provided for this discrepancy. Firstly, it is likely that the ideal intermittent contact model is too simple and further investigation is necessary to address this issue. Secondly, other parameters of the system may be oversimplified leading to miscalculations e.g. the value of N might be overestimated.

Figure 8 and Figure 6. show that there might be a correlation between the friction coefficient, and the measured acoustic force magnitude. This is explainable by taking into account that people with similar biomechanical finger propertie may have similar riction responses. Those with a high friction coefficient μ_{max} could have high acoustical finger forces, and vice versa. This can be explained, for example, by the moisture level of the participant's finger. Indeed, [6] demonstrates that higher level of moisture leads to higher level of friction coefficient, for all surfaces (without ultrasonic vibrations), while at the same time, [7] shows that a moist skin also has lower stiffness than a dry one, and thus needs higher vibration amplitude to obtain the intermittent contact. Two participants (7 and 10) however have higher coefficient of friction than what is expected from the proposed model. However, it can be observed that the behaviour of $\bar{F}_r$ in their case is different: it does not saturate, as if the finger skin had not reached the intermittent contact.

Finally, a PCA analysis was made in order to find out if the human parameter could be separated from the plate's vibration amplitude on the force response. Since this was the case, it was intended to find out whether the found parameters could be correlated to friction. It has been found out that a fair correlation can be established by only measuring one or two points of a single person, with the use of the statistical model obtained from the PCA.

8 Conclusion

A statistical model has been proposed to predict the maximum friction coefficient and the friction contrast for a subject touching a vibrating plate, from the observation of the fundamental acoustical force of the person's. The algorithms built from these models allow lesser processing hardware specifications than already proposed solutions, and minimize the amount of sensors required. They could therefore be implemented in real time on a light digital signal processor. Thanks to the aforementioned models, and the use of closed loop amplitude control, the level of vibration in ultrasonic haptic interfaces could be made to adapt to a given user, by only measuring one or two datapoints of this subject once. This result helps producing a more standardized sensation, by rendering these devices less dependent on finger bio-mechanics, hence more efficient from a haptic interaction point of view.

Acknowledgment

This work has been carried out within the framework of the Mint Project of IRCICA (CNRS Service and Research Unit 3380).

References

[1] L. Winfield, J. Glassmire, J. E. Colgate, and M. Peshkin, "T-PaD: Tactile Pattern Display through Variable Friction Reduction," *Second Joint EuroHaptics Conference and Symposium on Haptic Interfaces for Virtual Environment and Teleoperator Systems (WHC'07),* Tsukuba, Japan, 2007, pp. 421–426, doi: 10.1109/WHC.2007.105.

[2] M. Biet, F. Giraud, and B. Lemaire-Semail, "Squeeze film effect for the design of an ultrasonic tactile plate," *IEEE Transactions on Ultrasonics, Ferroelectrics and Frequency Control*, vol. 54, no. 12, pp. 2678–2688, Dec. 2007, doi: 10.1109/TUFFC.2007.596.

[3] E. Vezzoli, Z. Vidrih, V. Giamundo, B. Lemaire-Semail, F. Giraud, T. Rodic, D. Peric, M. Adams., "Friction Reduction through Ultrasonic Vibration Part 1: Modelling Intermittent Contact," *IEEE Transactions on Haptics (ToH)*, vol. 10, no. 2, pp. 196–207, 2017, doi: 10.1109/TOH.2017.2671432

[4] M. Wiertlewski, R. F. Friesen, and J. E. Colgate, "Partial squeeze film levitation modulates fingertip friction," *Proceedings of the National Academy of Sciences of the United States of America*, vol. 113, no. 33, pp. 9210–9215, Aug. 2016, doi: 10.1073/pnas.1603908113.

[5] R. F. Friesen, M. Wiertlewski, and J. E. Colgate, "The Role of Damping in Ultrasonic Friction Reduction," *in IEEE Haptics Symposium 2016,* pp. 167–172.

[6] W. B. Messaoud, M.-A. Bueno, and B. Lemaire-Semail, "Relation between human perceived friction and finger friction characteristics," *Tribology International,* vol. 98, pp. 261–269, Jun. 2016, doi: 10.1016/j.triboint.2016.02.031.

[7] Y.M. Khurram Saleem,, C. Yilmaz, and C. Basdogan, "Psychophysical Evaluation of Change in Friction on an Ultrasonically-Actuated Touchscreen," *IEEE Transactions on Haptics*, vol. 11, no. 4, pp. 599–610, Oct. 2018, doi: 10.1109/TOH.2018.2830790

[8] J. Monnoyer, E. Diaz, C. Bourdin, and M. Wiertlewski, "Perception of Ultrasonic Switches Involves Large Discontinuity of the Mechanical Impedance," *IEEE Transactions on Haptics*, vol. 11, no. 4, pp. 579–589, Oct. 2018, doi: 10.1109/TOH.2018.2844186.

[9] F. Giraud, M. Amberg, and B. Lemaire-Semail, "Design and control of a haptic knob," *Sensors and Actuators A: Physical*, vol. 196, pp. 78–85, Jul. 2013, doi: 10.1016/j.sna.2013.03.012.

[10] S. Ghenna, F. Giraud, C. Giraud-Audine, and M. Amberg, "Vector Control of Piezoelectric Transducers and Ultrasonic Actuators," *IEEE Transactions on Industrial Electronics*, vol. 65, no. 6, pp. 4880–4888, Jun. 2018, doi: 10.1109/TIE.2017.2784350.

[11] S. Ghenna, F. Giraud, C. Giraud-Audine, M. Amberg, and B. Lemaire-Semail, "Modelling, identification and control of a Langevin transducer,"

2015 IEEE International Workshop of Electronics, Control, Measurement, Signals and their Application to Mechatronics (ECMSM), Liberec, Czech Republic, 2015, pp. 1–6, doi: 10.1109/ECMSM.2015.7208676.

[12] D. Gueorguiev, E. Vezzoli, A. Mouraux, B. Lemaire-Semail, and J.-L. Thonnard, "The tactile perception of transient changes in friction," *Journal of The Royal Society Interface*, vol. 14, no. 137, p. 20170641, Dec. 2017, doi: 10.1098/rsif.2017.0641.

[13] J. van Kuilenburg, M. A. Masen, and E. van der Heide, "Contact modelling of human skin: What value to use for the modulus of elasticity?," *Proceedings of the Institution of Mechanical Engineers, Part J: Journal of Engineering Tribology*, vol. 227, no. 4, pp. 349–361, Apr. 2013, doi: 10.1177/1350650112463307.

[14] W. Ben Messaoud, M. Amberg, B. Lemaire-Semail, F. Giraud, M.A. Bueno "*High fidelity closed loop controlled friction in SMARTTAC tactile stimulator*" The 17th Conference on Power Electronics and Applications, EPE'15-ECCE Europe, Genève, SUISSE, 09/2015